The crystal structure of FdxA, a 7Fe ferredoxin from *Mycobacterium smegmatis*

Stefano Ricagno[1], Matteo de Rosa[1], Alessandro Aliverti[1], Giuliana Zanetti[1] and Martino Bolognesi[1,2,*]

[1]Department of Biomolecular Sciences and Biotechnology, University of Milano, Via Celoria 26, 20133-Milano, Italy

[2]CNR-INFM, c/o Department of Biomolecular Sciences and Biotechnology, University of Milano, Via Celoria 26, 20133-Milano, Italy

Keywords: 7Fe ferredoxin, mycobacterial ferredoxin, electron transfer, Fe/S cluster, [4Fe-4S] cluster instability, protein structure, X-ray crystallography

* Corresponding Author:
c/o Department of Biomolecular Sciences and Biotechnology
University of Milano Via Celoria 26, 20133-Milano, Italy
Fax +39 02 5031 4895
e-mail: martino.bolognesi@unimi.it

Abbreviations:

MsFd, *Mycobacterium smegmatis* FdxA ferredoxin; AvFd, *Azotobacter vinelandii* 7Fe ferredoxin I; BsFd, *Bacillus schlegelii* 7Fe ferredoxin; PaFd, *Pseudomonas aeruginosa* 8Fe ferredoxin; TtFd, *Thermus thermophilus* 7Fe ferredoxin.

Abstract

Ferredoxins containing one or two [Fe-S] centers are electron carrier proteins involved in several metabolic pathways of key relevance. *Mycobacterium smegmatis* ferredoxin FdxA, and the orthologue ferredoxin from *Mycobacterium tuberculosis*, contain two clusters, one [3Fe-4S] and one [4Fe-4S] cluster. Following our previous studies on *M. tuberculosis* FrpA, the proposed reductase coupled to the mycobacterial ferredoxin, we focused our attention on FdxA from *M. smegmatis*, a stable 7Fe ferredoxin composed of 106 amino acids. We report here the crystal structure of FdxA at 1.6 Å resolution (R-factor 16.5 % R-free 20.2 %). Besides providing insight on protein architecture for a 106-residue ferredoxin, our crystallographic investigation highlights lability of the [4Fe-4S] center, that is shown to loose a Fe atom during the crystal growth stage. The FdxA ferredoxin three-dimensional structure here reported is a step forward in the study of the complex mycobacterial redox pathways.

Introduction

Ferredoxins (Fds) are small acidic proteins, containing one or two [Fe-S] clusters. Three kinds of clusters have been described so far in Fds: [2Fe-2S], [3Fe-4S] and [4Fe-4S]. All Fds bearing any of such [Fe-S] clusters act as single–electron carriers in several key metabolic pathways. The 7Fe Fds are present apparently only in bacteria, and display both a cuboidal [3Fe-4S] cluster (cluster I), and a cubane [4Fe-4S] cluster (cluster II) within the same polypeptide chain. The genome of *Mycobacterium tuberculosis* encodes two 7Fe and three 3Fe Fds, respectively [1]. The two 7Fe Fds are held to be crucial for this pathogen: in particular FdxC was shown to be essential for optimal growth of the *mycobacterium* [2], whereas FdxA was reported to be induced under conditions of hypoxia and at low pH [3] , *i.e.* under conditions mimicking the environment of the infecting pathogen within macrophages [4].

In a search for potential protein targets for the design of novel drugs against tuberculosis, FprA, a *M. tuberculosis* adrenodoxin reductase-like enzyme, was functionally and structurally characterized [5, 6]. It is worth recalling that in mammals adrenodoxin reductases transfer electrons, by means of a 2Fe Fd, from NADPH to cytochrome P450s that are involved in key lipid metabolisms; it is also known that *M. tuberculosis* hosts twenty different cytochrome P450s [1]. On these bases, 3Fe and 7Fe Fds from *M. tuberculosis*, that are the presumed physiological substrates of FprA, were therefore overexpressed in

Escherichia coli, as possible new drug targets. Unfortunately, however, both recombinant Fds failed to yield the functional holoproteins. Thus, we resorted to using the 7Fe Fd of *Mycobacterium smegmatis* (FdxA, here referred to as MsFd), whose purification as an active recombinant protein had been reported [7]. The purified MsFd indeed proved to be a very good substrate for FprA, binding the reductase with high affinity [6]. In fact, the protein sequence comparison reported in Fig. 1 highlights the high similarity linking MsFd and *M. tuberculosis* FdxC, whith 87% amino acid identity and several conservative residue substitutions.

To date, four three-dimensional structures of 7Fe Fds have been elucidated. The structure of the *Azotobacter vinelandii* 7Fe Fd (avFd) was the first described, and currently the most thoroughly characterized by means of X-ray crystallographic, electrochemical and spectroscopic methods [8]. More recently, the 7Fe Fds from *Sulfolobus* sp. strain 7, *Thermus thermophilus* (TtFd) and *Bacillus schlegelii* (BsFd) have been reported [9-11]. Several 8Fe Fds three-dimensional structures are also available (Table 1). 7Fe and 8Fe Fds can vary in their size from about 55 to 105 amino acids. However, they all share a very similar [Fe-S] cluster binding core of about 55 amino acids, usually located at the N-terminus and folded according to a conserved $(\beta\alpha\beta)_2$ structure topology. The location of the two [Fe-S] clusters within the binding core is also conserved in 7Fe and 8Fe Fds. Interestingly, the same α-β fold is found in 4Fe Fds. On the other hand, outside the cluster binding core, all Fds show a higher level of structural variability.

Here we present the 1.6 Å resolution crystal structure of MsFd, the first mycobacterial Fd structure to be reported, and analyze its main structural features at the light of known three-dimensional structures of homologous 7Fe Fds. Our data unambiguously show that one Fe atom of the [4Fe-4S] cluster is not present in the crystallized MsFd, suggesting inherent instability of cluster II, that may have undergone a limited oxidative damage during the time required for crystal growth.

Materials and Methods

a) Purification of MsFd

Cells were grown at 37 °C for about 36 h in LB medium supplemented with 0.5 % (v/v) glycerol and 0.05 % (v/v) Tween 80. MsFd was purified according to the protocol

published by Imai *et al*. [7], modified as reported in [6]. Moreover, residual contaminant RNA was removed by a treatment with 0.1 mg/ml RNase I for 1 h, followed by a chromatography on a MonoQ 5/50 GL column (GE Healthcare), using a 0-1 M NaCl linear gradient. Finally, the protein was desalted by gel filtration in 50 mM Tris-HCl, pH 7.4, 0.2 M NaCl. The purified protein showed a single band in SDS-PAGE and an absorbance ratio (A_{406}/A_{280}) of 0.6. The protein concentration was determined spectrophotometrically using the reported extinction coefficient of 26 mM^{-1} cm^{-1}, at 406 nm [7].

b) Crystallisation

MsFd solution was concentrated by ultrafiltration (Centricon YM3) to a final concentration of 10 mg/ml. In initial crystal screenings, the use of different commercial kits resulted in the identification of crystal hits after 10 weeks in 3.5 M ammonium sulfate, 100 mM MES, pH 6.5, 1% 2-methyl-2,4-pentanediol (D5 condition from JBScreen classic 6, Jena bioscience). This crystal hit was further optimized to 3.4 M ammonium sulphate, 1% 2-methyl-2,4-pentanediol, 100 mM sodium acetate, pH 5.5. All crystallisations were performed at 20 °C. While the first screenings were carried out using the Oryx 8 crystallisation robot (Douglas Instruments Ltd., UK) in sitting drop plates, the final optimisation was achieved by manual crystallisation using the hanging drop technique. MsFd crystallised as dark red rods (about 0.5-1 mm long). The crystals were very fragile and were severely damaged by most cryoprotectant solutions; paraffin oil immersion was finally adopted as the cryoprotectant procedure. Two diffraction data sets were collected at 110 K, on the same crystal, at the European Synchrotron Radiation Facility (Grenoble) on beam lines ID23A and ID14-3. The first data set was collected at the peak of anomalous scattering for Fe (λ = 1.734 Å), at 2.15 Å resolution; the second at the remote wavelength λ = 0.931 Å, at 1.6 Å resolution. Analysis of the diffraction data showed that the MsFd crystals belong to the orthorhombic space group $C222_1$, with unit cell parameters: a = 54.8 Å, b = 54.3 Å, c = 134.7 Å, β = 90°, with two molecules in the asymmetric unit and a solvent content of 46%. Diffraction data were processed with MOSFLM/SCALA [12, 13].

c) Structure determination and refinement

The MsFd structure was solved by molecular replacement using the Fd of *Thermus thermophilus* (pdb 1H98) [11] as search model and the program MOLREP [14]. Model building and structure inspection were carried out using COOT [15]. The structure was then

refined with REFMAC5 [16] using the maximum likelihood residual, anisotropic scaling, bulk-solvent correction, and atomic displacement parameter refinement using the 'translation, libration, screw-rotation' method, treating each MsFd chain and every cluster as a rigid group. Anomalous maps were calculated with FFT in the CCP4 suite [13]. The MsFd structure was refined at 1.6 Å resolution to a final R-factor value of 16.5 % (R-free 20.2 %) with excellent stereochemical statistics; Table 2 lists the data collection and refinement statistics. Structure alignments were made with SSM [17]. Figures were drawn using Pymol (DeLano Scientific, South San Franciso, CA) and CCP4MG [18].

Atomic coordinates and structure factors for MsFd have been deposited in Protein Data Bank (pdbcode XXX).

Results

Overall structure of MsFd

MsFd is a monomer of 106 amino acids containing one [3Fe-4S] cluster and one [4Fe-4S] cluster. Two independent protein chains (A and B) are present in the crystallographic asymmetric unit, for which 104 and 103 amino acids could be modelled in the electron density, respectively. The electron density is of good quality for both chains and the amino acidic sequence could be unambiguously traced, yielding a high quality model as judged by stereochemical/crystallographic criteria (Table 2). The C-terminal amino acids for which electron density was missing are solvent exposed (Glu105-Asp106 in chain A, and Gly104-Glu105-Asp106 in chain B) (Fig.2). Moreover, residual electron density located between residues Cys42 from both chains A and B was observed (Fig. 3a).

MsFd displays the typical $(\beta\alpha\beta)_2$ motif building the [Fe-S] cluster-binding region (residues Thr1-Glu57), consisting of two small, double-stranded, antiparallel β-sheets (β1-β4 and β2-β3) with two α-helices (α2 and α3) packed on one face of the β-sheets (Fig. 2). An additional short α-helix (α1) is present in the middle of loop A. A short α-helix (α4) follows strand β4; the longer α5 helix (residues 65-78) packs onto the opposite face of the β-sheets relative to α2 and α3. The 27 C-terminal amino acids are organised in a loop (loop G), interrupted by helix α6, lying on the surface of the [Fe-S] cluster-binding core (Fig. 2). Both [Fe-S] clusters are located between the two β-sheets and α1, α2, α3 helices. The [3Fe-4S] cluster (cluster I) is coordinated by Cys residues 8, 16, and 49, while cluster II [4Fe-4S] is

linked to Cys 20, 39, and 45. Both clusters are inaccessible to the solvent; in particular, cluster I is protected by residues Val11 and Leu32, whereas cluster II is shielded from solvent by the side chain of Tyr2.

Inspection of the MsFd refined electron density shows unexpectedly that in the crystallized structure one Fe atom is not present in cluster II. Furthermore, the side chain of Cys42, which normally coordinates the fourth Fe atom in the 7Fe and 8Fe Fds, is pointing away from cluster II towards the solvent and the neighbouring protein molecule in the crystal asymmetric unit. Such conformation adopted by Cys42 (in both A and B chains) matches part of the unexplained residual electron density observed during the refinement. Structural and sequence searches (DALI and BLAST) against the Protein Data Bank showed that AvFd, TtFd and BsFd are the three-dimensional structures that match most closely that of MsFd. All three Fds contain a [4Fe-4S] cluster whose Cys residues are conserved and essentially structured as in MsFd [9, 11, 19], while keeping all the four Fe atoms.

7Fe Fds are known to be thermo- and air-stable [Fe-S] protein. Nevertheless, some evidence of the conversion of the 7Fe Fd [4Fe-4S] cluster into a [3Fe-4S] cluster under particular conditions has been reported. The crystal structure of the 7Fe Fd from *Sulfolbus* sp strain 7 [20] clearly shows that the [4Fe-4S] cluster II is present in this protein as a [3Fe-4S] cluster. Furthermore, while isolating MsFd, Imai *et al*. [21] purified a second Fd species containing only six Fe atoms. Such 6Fe Fd species turned out to be a modified form of MsFd, which had underwent partial oxidative degradation during the rather long purification procedure [10, 21]. More recently, the recombinant 7Fe Fds of *Bacillus thermoproteolyticus* have been characterized, showing once more a conversion of cluster II to a [3Fe-4S] form. The crystal structure of one of these 6Fe modified Fds shows that the cysteine, corresponding to Cys42 in MsFd, beared a covalently bound molecule of coenzyme A through a disulfide bond [22]. Thus, under particular conditions, oxygen can destabilize the [4Fe-4S] cluster, resulting in the loss of one Fe atom and in a conformational change that regularly affects the second Cys residue of the cluster binding motif Cys-X_2-**Cys**-X_2-Cys; such reactive Cys residue (Cys42 in MsFd) reorients its side-chain towards the solvent and may form disulfide bonds or be further oxidized. Interestingly, such selective conversion of cluster II does not destabilize cluster I, nor has sizeable effects on the overall protein structure [21, 22]. It must additionally be recalled that in 7Fe Fds the redox functional role has been assigned to the [3Fe-4S] cluster I, whereas cluster II is believed to play only a structural function [23] [24].

The packing of two MsFd molecules in the crystal asymmetric unit brings Cys42 of chains A and B in close spatial proximity (Cα – Cα distance of 7.3 Å). As mentioned above,

the refined crystal structure shows significant residual electron density located between these two residues, roughly comparable to the density that one would expect for an intermolecular covalent cross-bridge (Fig. 3). The distance between the SD atoms of Cys42 of chains A and B is however 5.20 Å, thus ruling out the possibility of a direct covalent bond between the two SD atoms contributed by the two protein chains. To shed light on the chemical nature of such intermolecular cross-bridge we first calculated an anomalous difference map based on the Fe anomalous contribution; such electron density map promptly located 6 Fe atoms, but did not show any peak outside the two [Fe-S] clusters, excluding the presence of Fe atoms in the Cys42 cross-bridge. The extra density at residue 42 was then modelled as hydroxyl-Cys, or persulfide-Cys. In the first case residual electron density was present after refinement on the modelled oxygen atoms and between the two Cys residues; furthermore, the distance between the putative O atom and SD was 2.0 Å, *i.e.* too long for a S-O bond. When Cys42 was modelled as persulfide-Cys, it showed a good stereochemistry for the SD-SE bond (SE is the persulfide S atom), with a SD-SE bond length of 2.05 Å, the distance between the putative SE atoms provided by chains A and B being however 3.0 Å. Although some residual density was still visible between the two putative SE atoms, additional atoms could not modelled. The above observations therefore suggest that the extra electron density observed between the Cys42 residues from the A and B chains may represent differently modified/oriented Cys species (including persulphide Cys), that may originate from a combination of air oxidation during crystal growth and X-ray radiation damage (at λ = 1.734 Å).

Comparison with other ferredoxins

All 7Fe and 8Fe Fds are phylogenetically related [25]. They display a high degree of structural homology showing the same common cluster-binding core of about 55 amino acids, based on the $(\beta\alpha\beta)_2$ motif. The conservation of the cluster-binding core is evident at the primary and tertiary structure levels in all 7Fe and 8Fe Fds (Table 1). The shortest Fds consist essentially of the cluster-binding core, whereas Fds composed of about 75-80 amino acids display a C-terminal α-helix corresponding to α5 of MsFd; such a helix is a characteristic structural feature of 7Fe thermostable Fds [11] and it is easily superimposable in all 7Fe Fds. MsFd three-dimensional structure can be superimposed on 8Fe Fd structures only for the minimal 55-residue core (Table 1 and Fig 4). For example, the 8Fe Fd from *P. aeruginosa* presents a C-terminal helix, but this does not match the location of the α5 helix of MsFd (Fig. 4) [26]. 7Fe Fds from mesophilic bacteria are often characterized by 30 C-terminal amino acids

following the α5 helix [11]; to date the structure of 7Fe AvFd is the only one available within such class [19]. MsFd and AvFd superimpose well for 85 residues, including the α5 helix. However, their C-terminal residues, consisting of a long loop and an α helix, are not superimposable and contact different sites of the Fd core (Table 1 and Fig. 4). While the cluster binding core is sufficient for the effective binding of two [Fe-S] clusters, the function of the C-terminal extension remains elusive, despite the extensive characterization of AvFd [27]. At the light of its sequence and structural variability, it can be speculated that the C-terminal region may be crucial for the interaction of MsFd with either its reductase or its electron acceptor(s). Experimental evidence in this direction is however lacking. It seems less likely that the C-termini of MsFd and AvFd might play any role in tuning the protein redox potentials, since they are not involved in interactions with the [Fe-S] clusters.

As mentioned above, MsFd displays 87% amino acid sequence identity with *M. tuberculosis* FdxC (Fig. 1). Since the similarity between the two Fds is very high, the crystal structure here presented may be regarded as a reliable model for *M. tuberculosis* FdxC. In our previous studies, MsFd has been identified, among various Fds, as the best electron-acceptor substrate of *M. tuberculosis* FprA [6]. Thus, it has been suggested that the *M. tuberculosis* FprA/FdxC system could provide reducing equivalents to (at least) some of the many cytochromes P450 of the pathogen. In this respect, the structure of MsFd is one further step in the direction of gaining insight on *M. tuberculosis* metabolic-redox pathways.

Acknowledgements

This work was supported by grants from … , from Fondazione Cariplo, Milano, Italy and MIUR (Prin 2005). S.R. is a youg-research-fellow of the MIUR Project "Biologia Strutturale" (FIRB 2003). M.B. is grateful to CIMAINA (Excellence Center, University of Milano) for continuous support. Drs Gerlind Sulzenbacher (Marseille) and Raffaele Cerutti (…….) are gratefully acknowledged for technical help.

References

[1] S.T. Cole, R. Brosch, J. Parkhill, T. Garnier, C. Churcher, D. Harris, S.V. Gordon, K. Eiglmeier, S. Gas, C.E. Barry, 3rd, F. Tekaia, K. Badcock, D. Basham, D. Brown, T. Chillingworth, R. Connor, R. Davies, K. Devlin, T. Feltwell, S. Gentles, N. Hamlin, S. Holroyd, T. Hornsby, K. Jagels, A. Krogh, J. McLean, S. Moule, L. Murphy, K. Oliver, J. Osborne, M.A. Quail, M.A. Rajandream, J. Rogers, S. Rutter, K. Seeger, J. Skelton, R. Squares, S. Squares, J.E. Sulston, K. Taylor, S. Whitehead, B.G. Barrell, Deciphering the biology of Mycobacterium tuberculosis from the complete genome sequence, Nature 393 (1998) 537-544.
[2] C.M. Sassetti, D.H. Boyd, E.J. Rubin, Genes required for mycobacterial growth defined by high density mutagenesis, Mol Microbiol 48 (2003) 77-84.
[3] D.R. Sherman, M. Voskuil, D. Schnappinger, R. Liao, M.I. Harrell, G.K. Schoolnik, Regulation of the Mycobacterium tuberculosis hypoxic response gene encoding alpha - crystallin, Proc Natl Acad Sci U S A 98 (2001) 7534-7539.
[4] H.D. Park, K.M. Guinn, M.I. Harrell, R. Liao, M.I. Voskuil, M. Tompa, G.K. Schoolnik, D.R. Sherman, Rv3133c/dosR is a transcription factor that mediates the hypoxic response of Mycobacterium tuberculosis, Mol Microbiol 48 (2003) 833-843.
[5] R.T. Bossi, A. Aliverti, D. Raimondi, F. Fischer, G. Zanetti, D. Ferrari, N. Tahallah, C.S. Maier, A.J. Heck, M. Rizzi, A. Mattevi, A covalent modification of NADP+ revealed by the atomic resolution structure of FprA, a Mycobacterium tuberculosis oxidoreductase, Biochemistry 41 (2002) 8807-8818.
[6] F. Fischer, D. Raimondi, A. Aliverti, G. Zanetti, Mycobacterium tuberculosis FprA, a novel bacterial NADPH-ferredoxin reductase, Eur J Biochem 269 (2002) 3005-3013.
[7] T. Imai, T. Matsumoto, S. Ohta, D. Ohmori, K. Suzuki, J. Tanaka, M. Tsukioka, J. Tobari, Isolation and characterization of a ferredoxin from Mycobacterium smegmatis Takeo, Biochim Biophys Acta 743 (1983) 91-97.
[8] C.D. Stout, Refinement of the 7 Fe ferredoxin from Azotobacter vinelandii at 1.9 A resolution, J Mol Biol 205 (1989) 545-555.
[9] S. Aono, D. Bentrop, I. Bertini, A. Donaire, C. Luchinat, Y. Niikura, A. Rosato, Solution structure of the oxidized Fe7S8 ferredoxin from the thermophilic bacterium Bacillus schlegelii by 1H NMR spectroscopy, Biochemistry 37 (1998) 9812-9826.
[10] T. Iwasaki, E. Watanabe, D. Ohmori, T. Imai, A. Urushiyama, M. Akiyama, Y. Hayashi-Iwasaki, N.J. Cosper, R.A. Scott, Spectroscopic investigation of selective cluster conversion of archaeal zinc-containing ferredoxin from Sulfolobus sp. strain 7, J Biol Chem 275 (2000) 25391-25401.
[11] S. Macedo-Ribeiro, B.M. Martins, P.J. Pereira, G. Buse, R. Huber, T. Soulimane, New insights into the thermostability of bacterial ferredoxins: high-resolution crystal structure of the seven-iron ferredoxin from Thermus thermophilus, J Biol Inorg Chem 6 (2001) 663-674.
[12] A.G.W. Leslie, Recent changes to the MOSFLM package for processing film and image plate data, Joint CCP4 + ESF-EAMCB Newsletter on Protein Crystallography (1992).
[13] CCP4, The CCP4 suite: programs for protein crystallography, Acta Crystallogr D Biol Crystallogr 50 (1994) 760-763.
[14] A.A. Vagin, A. Teplyakov, MOLREP: an automated program for molecular replacement, Journal of Applied Crystallography (1997) 1022-1025.
[15] P. Emsley, K. Cowtan, Coot: model-building tools for molecular graphics, Acta Crystallogr D Biol Crystallogr 60 (2004) 2126-2132.
[16] G.N. Murshudov, A.A. Vagin, E.J. Dodson, Refinement of macromolecular structures by the maximum-likelihood method, Acta Crystallogr D Biol Crystallogr 53 (1997) 240-255.

[17] E. Krissinel, K. Henrick, Secondary-structure matching (SSM), a new tool for fast protein structure alignment in three dimensions, Acta Crystallogr D Biol Crystallogr 60 (2004) 2256-2268.
[18] L. Potterton, S. McNicholas, E. Krissinel, J. Gruber, K. Cowtan, P. Emsley, G.N. Murshudov, S. Cohen, A. Perrakis, M. Noble, Developments in the CCP4 molecular-graphics project, Acta Crystallogr D Biol Crystallogr 60 (2004) 2288-2294.
[19] C.D. Stout, E.A. Stura, D.E. McRee, Structure of Azotobacter vinelandii 7Fe ferredoxin at 1.35 A resolution and determination of the [Fe-S] bonds with 0.01 A accuracy, J Mol Biol 278 (1998) 629-639.
[20] T. Fujii, Y. Hata, T. Wakagi, N. Tanaka, T. Oshima, Novel zinc-binding centre in thermoacidophilic archaeal ferredoxins, Nat Struct Biol 3 (1996) 834-837.
[21] T. Imai, A. Urushiyama, H. Saito, Y. Sakamoto, K. Ota, D. Ohmori, A novel 6Fe (2 x [3Fe-4S]) ferredoxin from Mycobacterium smegmatis, FEBS Lett 368 (1995) 23-26.
[22] T. Shirakawa, Y. Takahashi, K. Wada, J. Hirota, T. Takao, D. Ohmori, K. Fukuyama, Identification of variant molecules of Bacillus thermoproteolyticus ferredoxin: crystal structure reveals bound coenzyme A and an unexpected [3Fe-4S] cluster associated with a canonical [4Fe-4S] ligand motif, Biochemistry 44 (2005) 12402-12410.
[23] T. Iwasaki, T. Wakagi, Y. Isogai, K. Tanaka, T. Iizuka, T. Oshima, Functional and evolutionary implications of a [3Fe-4S] cluster of the dicluster-type ferredoxin from the thermoacidophilic archaeon, Sulfolobus sp. strain 7, J Biol Chem 269 (1994) 29444-29450.
[24] C.D. Stout, Ferredoxins containing two different Fe/S centers of the forms [4Fe-4S] and [3Fe-4S] in: A. Messerschmidt, Huber, R., Poulos, T., Wieghardt, K. (Eds.), Handbook of Metalloproteins, Wiley & sons, ltd, Chichester, 2001, pp. 560-574.
[25] K. Fukuyama, H. Matsubara, T. Tsukihara, Y. Katsube, Structure of [4Fe-4S] ferredoxin from Bacillus thermoproteolyticus refined at 2.3 A resolution. Structural comparisons of bacterial ferredoxins, J Mol Biol 210 (1989) 383-398.
[26] P. Giastas, N. Pinotsis, G. Efthymiou, M. Wilmanns, P. Kyritsis, J.M. Moulis, I.M. Mavridis, The structure of the 2[4Fe-4S] ferredoxin from Pseudomonas aeruginosa at 1.32-A resolution: comparison with other high-resolution structures of ferredoxins and contributing structural features to reduction potential values, J Biol Inorg Chem 11 (2006) 445-458.
[27] Y.S. Jung, V.A. Roberts, C.D. Stout, B.K. Burgess, Complex formation between Azotobacter vinelandii ferredoxin I and its physiological electron donor NADPH-ferredoxin reductase, J Biol Chem 274 (1999) 2978-2987.
[28] E.T. Adman, L.C. Siefker, L.H. Jensen, Structure of Peptococcus aerogenes ferredoxin. Refinement at 2 A resolution, J Biol Chem 251 (1976) 3801-3806.
[29] I. Bertini, A. Donaire, B.A. Feinberg, C. Luchinat, M. Piccioli, H. Yuan, Solution structure of the oxidized 2[4Fe-4S] ferredoxin from Clostridium pasteurianum, Eur J Biochem 232 (1995) 192-205.
[30] Z. Dauter, K.S. Wilson, L.C. Sieker, J. Meyer, J.M. Moulis, Atomic resolution (0.94 A) structure of Clostridium acidurici ferredoxin. Detailed geometry of [4Fe-4S] clusters in a protein, Biochemistry 36 (1997) 16065-16073.
[31] J.M. Moulis, L.C. Sieker, K.S. Wilson, Z. Dauter, Crystal structure of the 2[4Fe-4S] ferredoxin from Chromatium vinosum: evolutionary and mechanistic inferences for [3/4Fe-4S] ferredoxins, Protein Sci 5 (1996) 1765-1775.
[32] M. Unciuleac, M. Boll, E. Warkentin, U. Ermler, Crystallization of 4-hydroxybenzoyl-CoA reductase and the structure of its electron donor ferredoxin, Acta Crystallogr D Biol Crystallogr 60 (2004) 388-391.

Table 1: List of 7Fe and 8Fe Fds of known three-dimensional structure. The fourth column lists the RMSD values obtained after superimposition of each FD structure with MsFd (in parentheses the number of matched Cα pairs).

[Fe-S] clusters	Organism PDB code	Resolution (Å)	RMSD (AA aligned)	Seq. length	Reference
[4Fe–4S] [3Fe–4S]	*M. smegmatis* *This work*	1.60 Å	-	106	This work
[4Fe–4S] [3Fe–4S]	*A. vinelandi* *6FD1*	1.35 Å	1.9 Å (85)	106	[19]
[4Fe–4S] [3Fe–4S]	*T. thermophilus* *1H98*	1.64 Å	0.6 Å (77)	77	[11]
[4Fe–4S] [3Fe–4S]	*B. schlegelli* *1BD6*	NMR	1.8 Å (77)	77	[9]
[3Fe–4S] [3Fe–4S] Zn	*Sulfolobus* strain 7 1XER	2.00 Å	1.8 Å (56)	103	[20]
Clostridial 2[4Fe–4S]	*P. asaccharolyticus* 1FDX/1DUR	2.0 Å	0.99 Å (55)	55	[28]
Clostridial 2[4Fe–4S]	*C. pasteurianum* *1CLF*	NMR	2.0 Å (55)	55	[29]
Clostridial 2[4Fe–4S]	*C. acidurici* *2FDN*	0.94 Å	1.1 Å (55)	55	[30]
Alvin-like 2[4Fe–4S]	*A. vinosum* 1BLU	2.1 Å	1.02 Å (55)	80	[31]
Alvin-like 2[4Fe–4S]	*T. aromatica* 1RGV	2.9 Å	1.99 Å (30)	80	[32]
Alvin-like 2[4Fe–4S]	*P. aeruginosa* *2FGO*	1.32 Å	2.0 Å (55)	81	[26]

Table 2 - Data collection and refinement statistics for MsFd

DATA COLLECTION	Remote dataset	Fe peak
Wavelength (Å)	0.931	1.734
Beam line (ESRF)	ID23-A	ID14-1
Cell dimensions (Å)	a=54.8 b=54.28 c=134.7, $\alpha=\gamma=90$ $\beta=89.9^{o}$	
Resolution (Å)	38-1.60	67-2.15
R sym (%)	7.4 (33.9)	7.3 (3.29)
I/σI	12.9 (2.7)	11.5 (5.3)
Completeness (%)	93.9 (99.9)	95.4*
Redundancy	3.5 (3.5)	6.1*
Unique reflections	26692 (874)	10621 (1131)
REFINEMENT		
R work (%)	16.5	
R free (%)	20.2	
Number of atoms:		
Protein	1640	
Solvent	99	
Ramachandran plot		
Most favoured region	88.3 %	
Additional allowed region	11.7 %	
Generously allowed region	0.0 %	
Disallowed region	0.0 %	

Statistics in parentheses refer to the high resolution shell (1.60-1.69 Å for the remote dataset; 2.15-2.27 Å for the anomalous peak dataset). * Anomalous completeness and redundancy are givan.

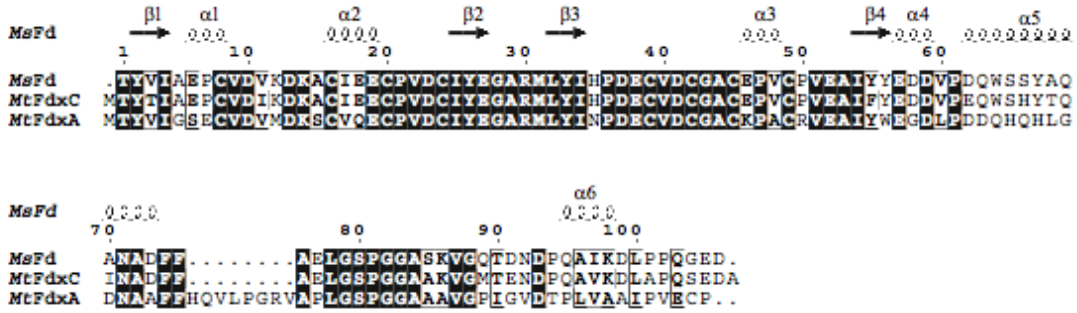

Figure 1: Sequence alignment of MsFd from *M. smegmatis* with FdxC and FdxA from *M. tuberculosis*. Secondary structure elements of MsFd are reported on top of the alignment.

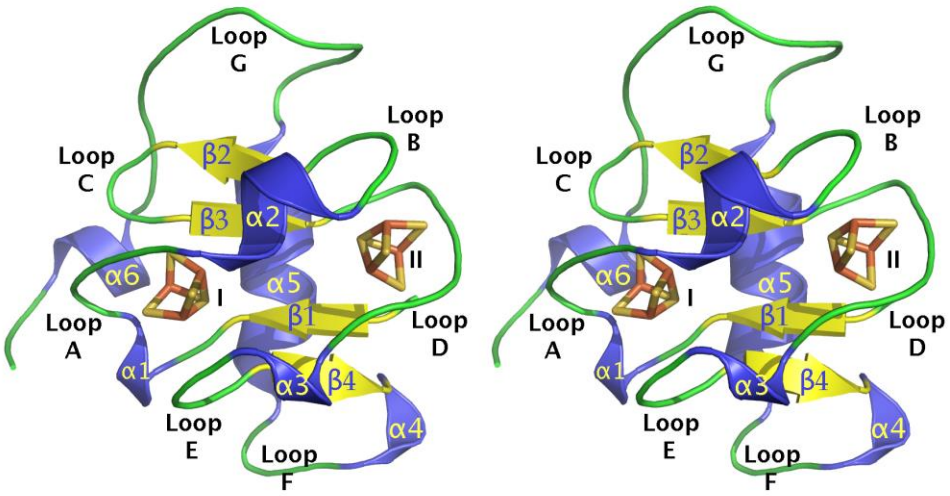

Figure 2: Cartoon representation of the 7Fe Fd of *M. smegmatis* in stereo view. The two [Fe-S] clusters are identified as I and II. All secondary structure elements and loops are labelled; α-helical regions are shown in blue, the β-strands in yellow..

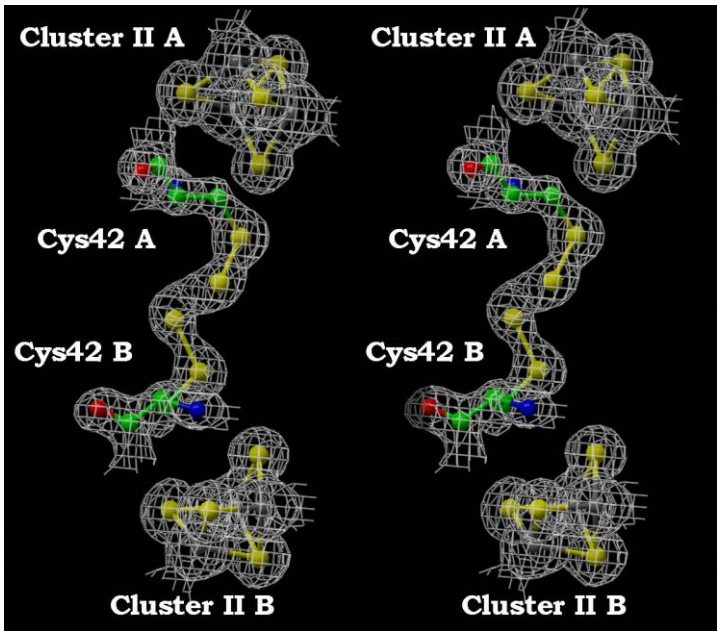

a)

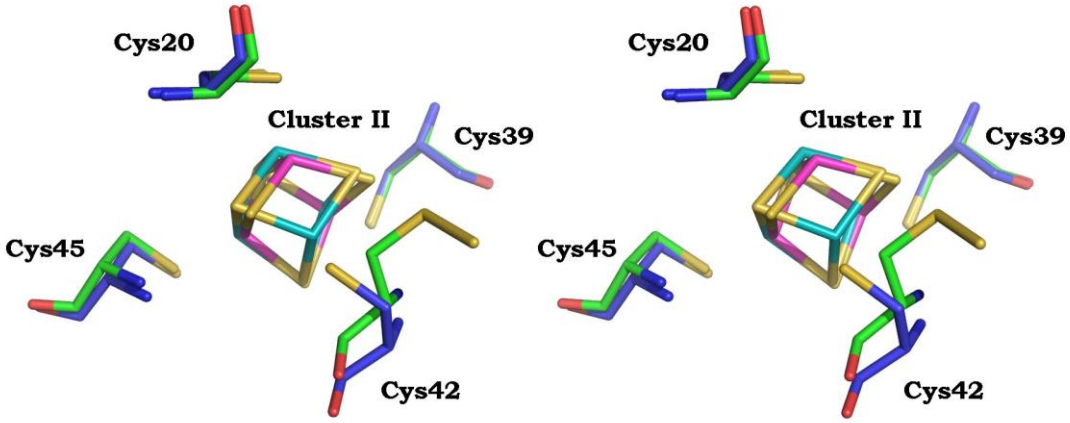

b)

Figure 3: a) Ball and stick representation of Cys42 and cluster II from molecules A and B. The electron density for the refined model (contoured at 1.5 σ) is shown. b) Superimposition of cluster II in MsFd (magenta) and TtFd (cyan). Cys residues coordinating cluster II from MsFd and TtFd are shown in blue and green, respectively; MsFd Cys42 has flipped away from cluster II, and the corresponding Fe atom is absent.

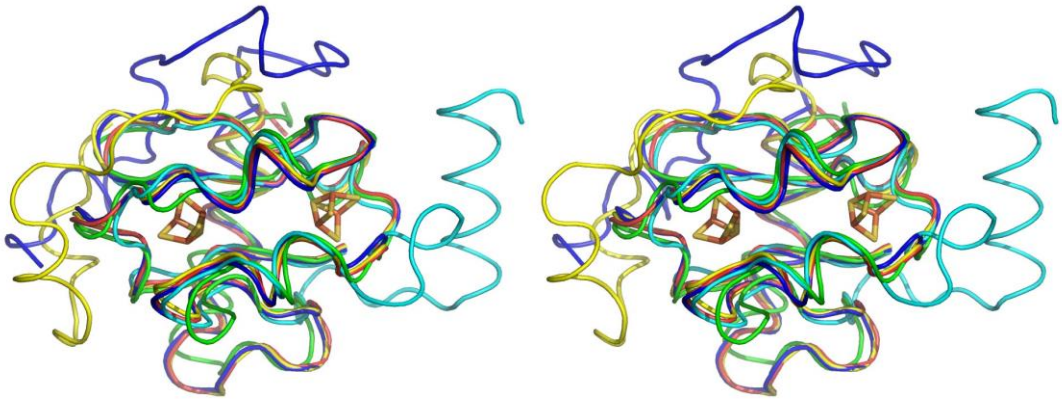

Figure 4: (a) Superimposition of MsFd (blue) with other 7Fe Fds: AvFd (yellow), BsFd (green), TtFd (red), and the 8Fe Fd PaFd (cyan). Only the MsFd [Fe-S] clusters are shown. BsFd and TtFd structures (77 amino acids long) match nicely, while PaFd displays a C-terminal helix differently oriented relative to the α5 helix. MsFd (blue) and AvFd (yellow) are well superimposed between amino acids 1 - 85, while the C-terminal 30 amino acids are entirely differently structured.